# Supporting Information

## Mouse Adapted MERS-Coronavirus

## Causes Lethal Lung Disease in Human DPP4 Knock-in Mice

Kun Li[1], Christine L. Wohlford-Lenane[1], Rudragouda Channappanavar[2], Jung-Eun Park[3], James T. Earnest[3], Thomas B. Bair[4], Amber M. Bates[5], Kim A. Brogden[5], Heather A. Flaherty[7], Tom Gallagher[3], David K. Meyerholz[6], Stanley Perlman[1,2], Paul B. McCray, Jr.[1,2]

[1]Department of Pediatrics, Pappajohn Biomedical Institute,

University of Iowa, Iowa City, IA 52242

[2]Department of Microbiology, University of Iowa, Iowa City, IA 52242

[4]Iowa Institute of Human Genetics, University of Iowa, Iowa City, IA 52242

[5]College of Dentistry, University of Iowa, Iowa City, IA 52242

[6]Department of Pathology, University of Iowa, Iowa City, IA 52242

[7]Department of Veterinary Pathology, Iowa State University, Ames, IA 50011

[3]Department of Microbiology and Immunology,

Loyola University Chicago, Maywood, IL, 60153

*Corresponding author: Paul McCray, Pappajohn Biomedical Institute, Department of Pediatrics, 6320 PBDB, University of Iowa, Iowa City, IA 52242, tel. 319-335-6844, Fax. 319-335-6925, Email: paul-mccray@uiowa.edu

**This PDF file includes:**
Materials and Methods

References



## MATERIALS AND METHODS

**Generation of mice with humanized exons 10-12 of the mouse *Dpp4* gene.** A congenic C57BL/6 mouse with mouse *Dpp4* exons 10-12 replaced with the human *DPP4* codons was generated by Taconic Biosciences (Cologne, Germany). This allowed the modified mouse gene product to display amino acids required for virus binding (1-3). The targeting strategy was based on NCBI transcripts NM_010074_3 (mouse) and NM_001935_3 (human). The targeting vector was generated using BAC clones from the mouse C57BL/6J RPCIB-731 and human RPCIB-753 BAC libraries. Mouse genomic sequence from codon I264 in exon 10 to codon V340 in exon 12 was replaced with its human counterpart. Positive selection markers were flanked by FRT (Neomycin resistance - NeoR) and F3 (Puromycin resistance - PuroR) sites and inserted into intron 9 and intron 12, respectively. The remaining recombination sites were located in non-conserved regions of the genome. Figure S1 shows the gene targeting strategy used to generate the human DPP4 knock in mice.

The targeting vector (pDpp4_Final_(AMX22983), 31,280 bp) was transfected into the

TaconicArtemis C57BL/6N Tac ES cell line. Homologous recombinant clones were isolated using double positive (NeoR and PuroR) and negative (Thymidine kinase - Tk) selections. The humanized allele was obtained after *in vivo* Flp-mediated removal of the selection marker. The chimeric mouse-human *DPP4* gene was expressed under the control of the endogenous mouse *Dpp4* promoter and should therefore recapitulate the expression pattern of the mouse gene.

Superovulated BALB/c females were mated with BALB/c males. Blastocysts were isolated from the uterus at dpc 3.5 and 10-15 targeted C57BL/6NTac ES cells injected into each blastocyst. After recovery, 8 injected blastocysts were transferred to each uterine horn of 2.5 days post coitum, pseudopregnant NMRI females. Chimerism was measured in chimeras (G0) by coat color contribution of ES cells to the BALB/c host (black/white). Highly chimeric mice were bred to strain C57BL/6 females. Germline transmission was identified by the presence of black, strain C57BL/6, offspring (G1). For the studies reported, we used mice homozygous for hDPP4. All studies were approved by the Animal Care and Use Committee of the University of Iowa.

To genotype animals, tail DNA was isolated using a Wizard SV Genomic Purification System (Promega). The humanized *DPP4* allele was detected by PCR analysis using the forward primer TCAATAATGTCCATTGCTCACC and reverse primer CCGTCCAGTTTTCATCTTCC.

**Cytokine and chemokine profiling by immunoassay.** Cytokine and chemokine levels were determined in lung tissue homogenates and serum using a commercial multiplexed fluorescent bead-based immunoassay (R&D Systems, Minneapolis, MN) and a Luminex 100 Instrument (Luminex, Austin TX). Each sample was assayed in duplicate. Briefly, for each replicate, 50 µl of lung homogenate or serum sample were incubated with anti-mouse multi-cytokine beads at 4°C on an orbital shaker (Titer Plate Shaker, Lab-Line Instruments, Inc., Melrose Park, IL USA).

After 18.0 hrs, culture media was removed by aspiration using an automated microtiter plate washer (ELx405TS magnetic plate washer, BioTek, Winooski, VT USA). Anti-mouse multi-cytokine biotin reporter was added, and reactions were incubated at room temperature for 1.5 hrs in the dark. The plate was then washed to remove excess biotin antibody. Streptavidin–phycoerythrin then was added, and the plates were incubated at room temperature for an additional 0.5 hr. The plate was washed to remove excess Streptavidin-PE. Median fluorescent intensity (MFI) values of the reporter on the multi-cytokine magnetic beads were determined in the Luminex model 100 IS (Luminex, Austin, TX USA). High and low quality controls were added to ensure the standard curve values fell within the detectable range. The concentrations of individual chemokine or cytokine values in each sample were interpolated from standard curves prepared by plotting concentrations of the known chemokine or cytokine standard versus its respective MFI value using xPonent v3.1 (Luminex, Austin, TX USA) and MILLIPLEX Analyst v5.1 (Millipore, Billerica, MA USA).

**MERS-CoV genome sequencing and assembly.** Viral RNA was isolated from producer cell supernatants using a QIAamp Viral RNA MiniKit (Qiagen) according to manufacturer's specifications. Viral cDNA was generated using Superscript III reverse transcriptase and a random hexamer priming approach. Specifically, 11 µl of total RNA was added to 1 µl of FR26RV-N, 1 µl of 10 mM dNTP mix, 4 µl of 5X First Strand Buffer, 1 µl of 0.1 M DTT, 1 µl of RNaseOUT, and 1 µl of Superscript III Reverse Transcriptase.

Second strand cDNA synthesis was carried out using the Sequenase 2.0 Kit. With nucleotides and primers still present from the previous reaction, it was only necessary to add an equal

volume of Sequenase and Sequenase buffer to the reaction tubes. The tubes were then placed in a thermocycler set to 4°C and ramped to 37°C at a rate of 0.1°C/s and then the samples were incubated at 37°C for 10 minutes, 95°C for 2 minutes and placed on ice. An additional volume of Sequenase was added to each reaction and the ramping program and incubation were repeated with the exception of increasing the 37°C incubation time to 30 minutes. The double stranded cDNA was then purified using Minelute PCR spin columns (Qiagen) according to manufacturer's specifications.

Double stranded cDNA was then amplified using the complementary forward primer to the random primer used in the reverse transcription reaction. The reaction consisted of 10 µl of double-stranded cDNA, 10 µl FR20RV primer, 1 µl of AmpliTaq Gold Polymerase, 5 µl of 10X PCR Buffer II, 2 µl of 10 mM dNTP mix, 3 µl of 25 mM $MgCl_2$, and ultra pure water for a total reaction volume of 50 µl. The amplified double-stranded cDNA was again purified using Minelute PCR spin columns and diluted to a concentration of 0.2 ng/µl.

The Nextera XT library preparation kit (Illumina) was used according to manufacturer's specifications to tagment the samples and add barcode indexes in a limited cycle PCR reaction. The samples were then normalized to 4 nM, pooled, and loaded onto an Illumina MiSeq bench top sequencer using a 300 cycle cartridge to produce 150 base pair, paired end reads.

The MERS-CoV genome (EMC/2012, JX869059.2) was downloaded from NCBI and used for alignment. Both the FASTA sequence and the GenBank file were used. The GenBank file was converted to GFF and used to annotate the sequence mapping. The FASTA file was used to

generate a BWA index for alignment. Bcbio (v 0.9.5) was used as a framework (4) to trim, align, and call variants. Basic quality control data was assessed using FastQC (v 0.11.4). FASTQ sequences were pre-processed using cutadapt (v 1.9.1). BWA-MEM (v 0.7.12) was used to align the data. Variant calling was done using FreeBayes (v 0.9.21.26) with the ploidy option set to 1. Rearrangements and deletions were first assessed with CNVkit (v 0.7.3) and then confirmed using visualization. Visualization was done using the IGV browser (v 2.3.67). Mapped read counts depths varied between 70-1,350 x $10^3$. Variant effects were predicted using SnpEff (v 4.1).

**MERSpp protease sensitivity and cell entry kinetics.** Murine lung epithelial type 1 (LET1) cells (4) were maintained in media (DMEM supplemented with 10% FBS, 100 U/ml penicillin, and 100 $\mu$g/ml streptomycin). The LET1 cells were sensitized to transduction by luciferase-encoding VSV-based MERS pseudo-particles (MERSpp) (5) through a prior transduction with recombinant Ad5 viruses expressing human DPP4 (6), at 10 $TCID_{50}$/cell. The Ad5-encoded hDPP4 was expressed for 4 days before cells were inoculated with MERSpp. To identify requirements for host proteases in MERSpp transduction, cells were treated with 0-1,000 $\mu$M camostat (Sigma-Aldrich), 0-1,000 $\mu$M E64D (Sigma-Aldrich), or DMSO vehicle, and MERSpp were inoculated 1h later. After a 2-h inoculation period, MERSpp and inhibitors were removed and replaced with media. To reveal kinetics of virus entry, cells were inoculated with MERSpp for 1h at 4ºC, then rinsed and overlaid at time t = 0 with 37ºC media. At the indicated post-transduction time points, a 37ºC-tempered protease inhibitor cocktail was added, to bring final concentrations of 100 $\mu$M camostat, 10 $\mu$M proprotein convertase inhibitor (Sigma-Aldrich), and 10 $\mu$M E64d. At 2 h post-transduction, MERSpp and inhibitors were removed and replaced with

media. In both experiments, cells were dissolved in passive lysis buffer (Promega) at 18 h post-transduction and luciferase reporter gene products were measured using a luciferin substrate (Promega) and a microplate luminometer (Veritas).

**References**


1. Lu G, *et al.* (2013) Molecular basis of binding between novel human coronavirus MERS-CoV and its receptor CD26. *Nature*. 500(7461):227-231.
2. Wang N, *et al.* (2013) Structure of MERS-CoV spike receptor-binding domain complexed with human receptor DPP4. *Cell Res*. 23(8):986-93.
3. Barlan A, *et al.* (2014) Receptor variation and susceptibility to Middle East respiratory syndrome coronavirus infection. *J. Virol.* 88(9):4953-4961.
4. Rosenberger CM, *et al.* (2014) Characterization of innate responses to influenza virus infection in a novel lung type I epithelial cell model. *J. Gen. Virol.* 95(Pt 2):350-362.
5. Park JE, *et al.* (2016) Proteolytic processing of Middle East respiratory syndrome coronavirus spikes expands virus tropism. *Proc. Natl. Acad. Sci. USA* 113(43):12262-12267.
6. Zhao J, *et al.* (2014) Rapid generation of a mouse model for Middle East respiratory syndrome. *Proc. Natl. Acad. Sci. USA*. 111(13):4970-4975.

## Supplemental Figures

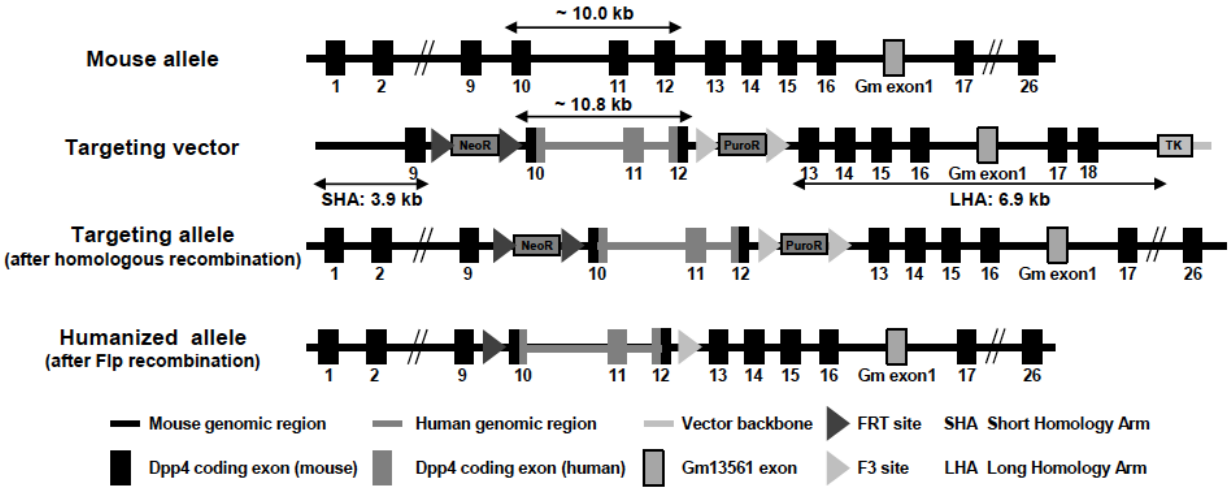


**Figure S1. Gene targeting strategy for generation of hDPP4 knock-in mice.** Top line depicts the native mouse *Dpp4* locus. The native DPP4 exons are indicated by black rectangles. "Gm exon 1" denotes a neighboring gene. The second line shows a schematic diagram of the targeting construct to modify the mouse *Dpp4* locus. The third line depicts the mouse *Dpp4* locus following homologous recombination. The bottom line shows the modified locus after Flp recombination.

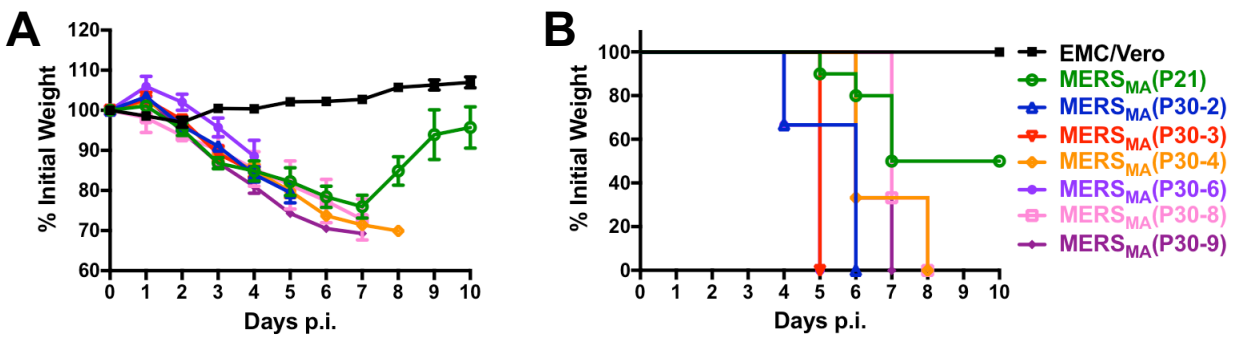


**Figure S2. Outcomes in hDPP4 KI mice infected with EMC/Vero, passage 21 $MERS_{MA}$ (P21), and 6 different passage 30 $MERS_{MA}$ isolates (P30-X).** Weight loss (A) and survival (B) in KI mice infected i.n. with $10^5$ pfu of indicated virus. EMC/Vero infected mice had 100% survival. KI mice infected with P21 $MERS_{MA}$ lost significant weight and had ~50% mortality. Six of nine plaque-purified isolates were evaluated in KI mice at a $10^5$ pfu inoculum and each caused fatal disease. n=6 (EMC/Vero), n=10 (P21 $MERS_{MA}$), n=3 (P30-X $MERS_{MA}$ plaque purified virus); Mixed male and female mice; mixed ages.

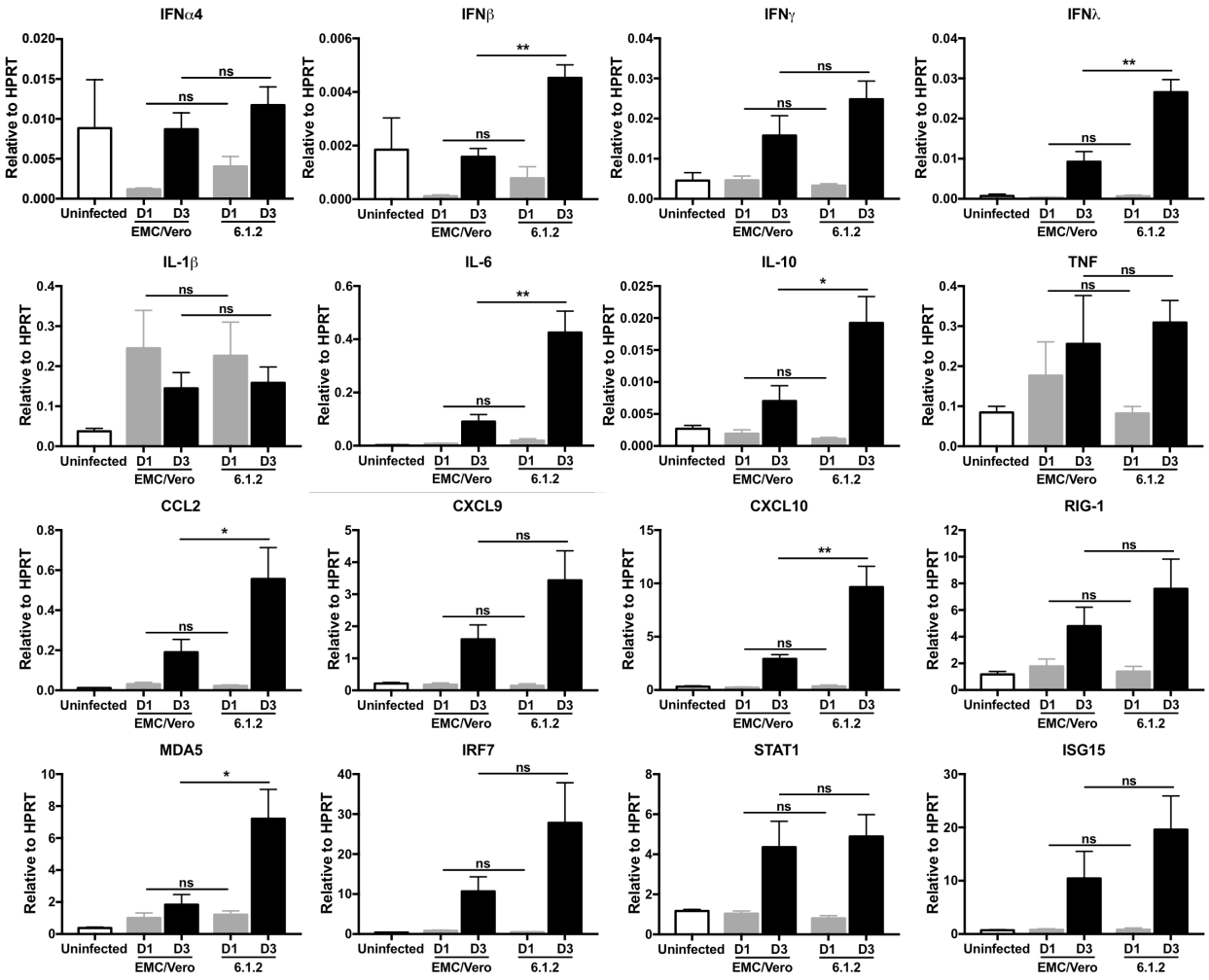


**Figure S3. Interferon, cytokine, chemokine, and interferon stimulated gene mRNA transcript responses to EMC/Vero or $MERS_{MA}$ clone 6.1.2 (6.1.2) infection in hDPP4 KI mice.** Lung tissues were harvested 1 and 3 d.p.i. following i.n. inoculation with indicated virus ($10^4$ inoculum). RNA was prepared from lungs and assayed for indicated mRNA levels using qRT-PCR as described in Methods. Data are presented as mRNA abundance normalized to the level of HPRT, mean ± SE. n=6-7 mice/group, representative of 2 replicate experiments. * $P < 0.05$, ** $P < 0.01$. ns = not significant.

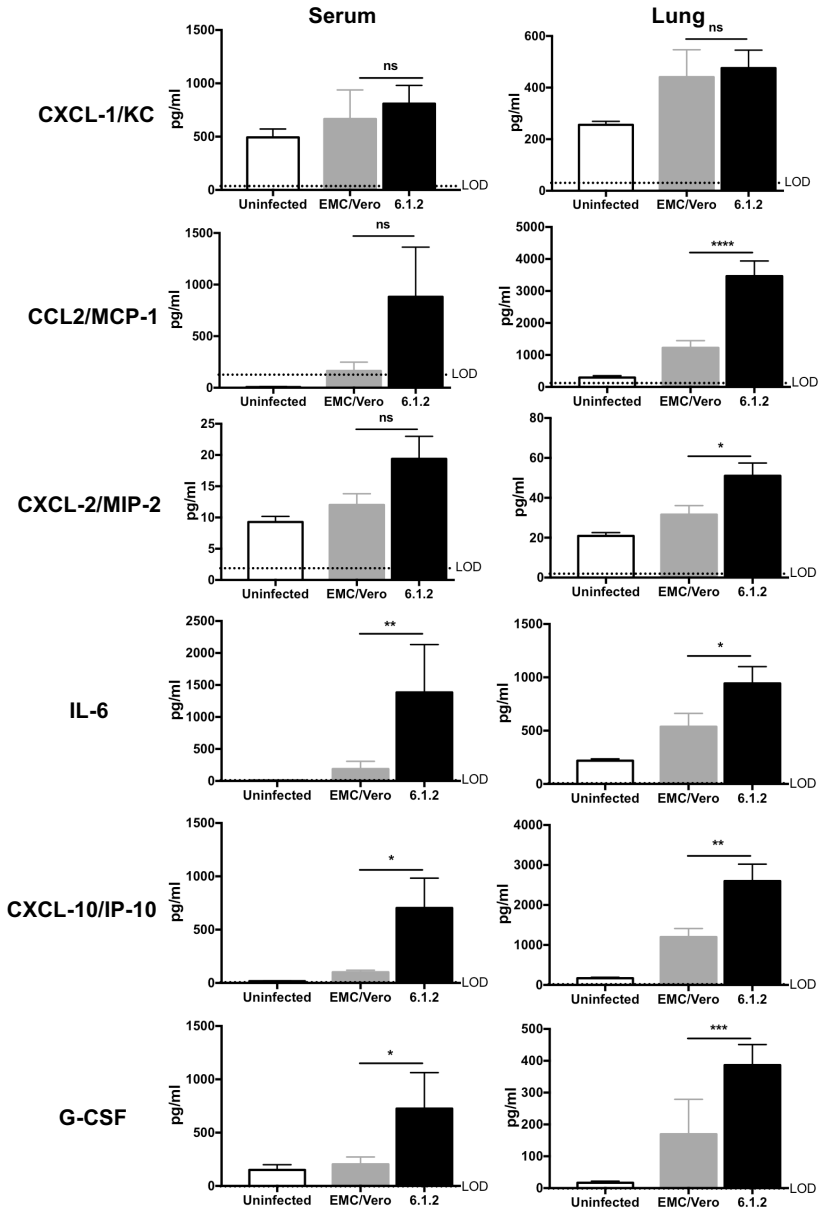


**Figure S4. Serum and lung tissue cytokine and chemokine protein responses to EMC/Vero or MERS$_{MA}$ clone 6.1.2 (6.1.2) infection in hDPP4 KI mice.** Serum and lung tissues were harvested 3 d.p.i. following i.n. inoculation with indicated virus ($10^4$ inoculum). Samples were prepared for analysis as described in Methods. Data are presented as protein abundance in pg or ng/ml as indicated, mean ± SE. n=5-8 mice/group, representative of 2 replicate experiments. * P < 0.05, ** P< 0.01, *** P< 0.001. ns = not significant.

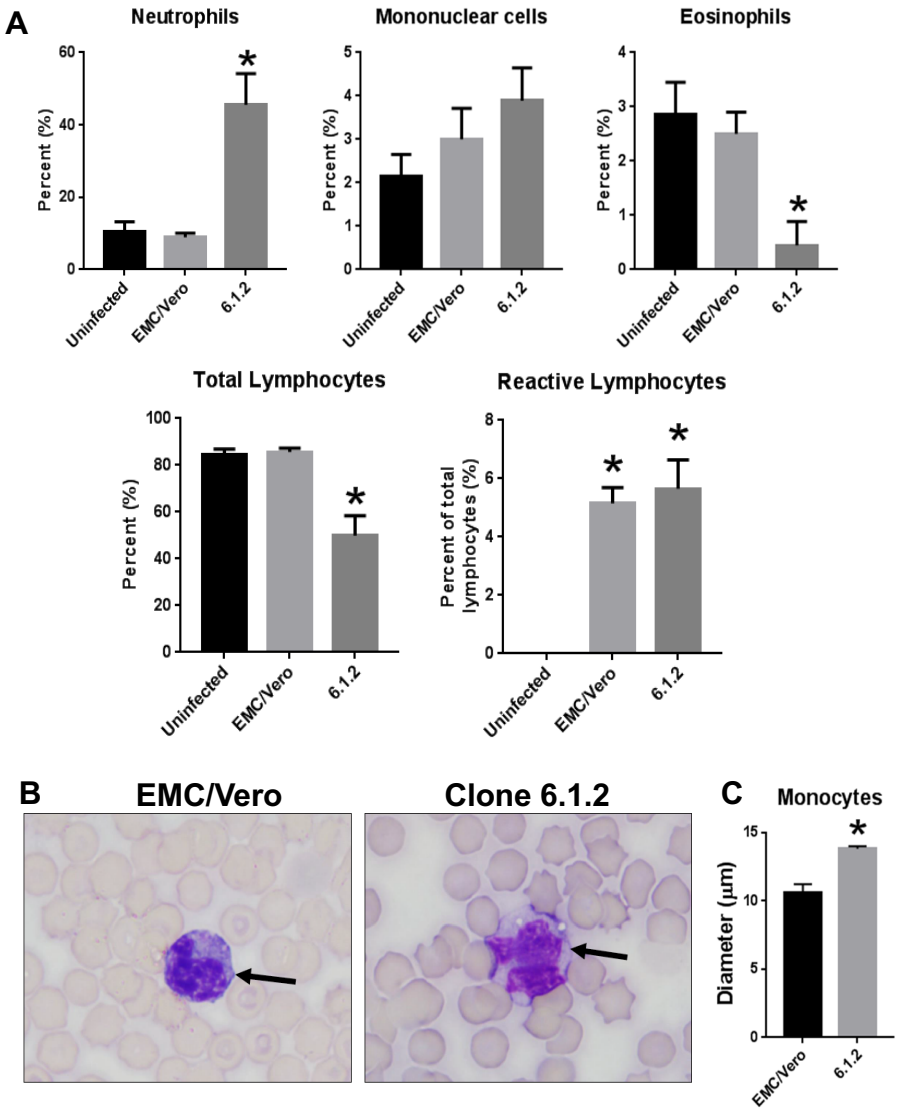


**Figure S5. Effects of EMC/Vero and MERS$_{MA}$ clone 6.1.2 infection on peripheral blood cells.** Samples were collected at 3 and 4 d.p.i. as described in Methods. A) Quantification of percentage of indicated cell types in peripheral blood. (*$P$< 0.05, Dunn's Multiple Comparison test). B) Monocytes (arrows) from peripheral blood smears. Compared to EMC/Vero infected mice, clone 6.1.2 animals had more circulating monocytes with evidence of activation as evidenced by increased diameter and less condensed chromatin. Blood smears from clone 6.1.2 also had reduced erythrocyte density and reduced polychromatophils (immature RBCs)

consistent with anemia of inflammation. C) Morphometric evaluation of monocytes showed a significant increase in size (*$P$=0.0006, Mann Whitney test). n= 7-9 mice per group.

**A**

**Mutations identified in 9 single plaque purified $MERS_{MA}$**

| ORF | Plaque # 1 | 2 | 3 | 4 | 5 | 6 | 7 | 8 | 9 |
|---|---|---|---|---|---|---|---|---|---|
| **1a** | | | | | | | | | |
| **-nsp3** | 1* | 2* | 3* | 2* | 1* | 1* | 1* | 1* | 1* |
| **-nsp4** | | 1* | | 1* | 1* | | | 1* | 1* |
| **-nsp5** | 1* | 1* | | | 1* | 1* | 1* | 1* | 1* |
| **-nsp6** | | | 1* | 2* | | 1* | | | |
| **-nsp9** | 1* | 1* | 1* | 1* | 1* | 1* | 1* | 1* | 1* |
| **1b** | | | | | | | | | |
| **-nsp14** | 1* | 1* | 1* | 1* | 1* | 1* | 1* | 1* | 1* |
| **S** | 2* | 3* | 3* | 3* | 3* | 2* | 4* | 3* | 3* |
| **3** | | 1# | 1# | 1# | 1# | | 1# | 1# | 1# |
| | | 1* | 1* | 1* | 1* | | 1* | 1* | 1* |
| **4a** | | 1# | 1# | 1# | 1# | | 1# | 1# | 1# |
| | | 1* | 1* | 1* | 1* | | 1* | 1* | |
| **4b** | | 1# | 1# | 1# | 1# | | 1# | 1# | 1# |
| | 1* | 2* | 1* | 2* | 2* | 1* | 1* | 2* | 1* |
| **5** | 1# | | | | | 1# | 1# | | |
| | 1* | 1* | 1* | 1* | 1* | 1* | 1* | 1* | 1* |
| **M** | 1* | 1* | 1* | 1* | 1* | 1* | 1* | 1* | 1* |
| **N** | 2* | 1* | 2* | 2* | | 1* | 1* | 2* | 2* |

**Type of Mutation: *Missense or nonsense, #Deletion**

**B**

**Mutations identified in $MERS_{MA}$ clone 6.1.2**

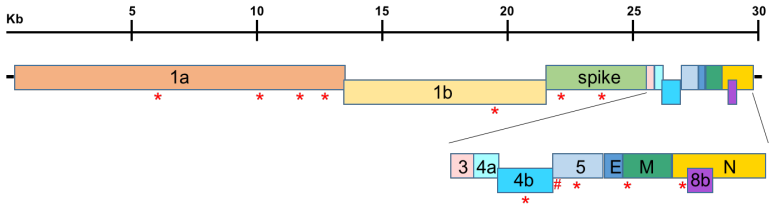


**C**

**Mutations found in $MERS_{MA}$ clone 6.1.2 compared to MERS-CoV (EMC/2012)**

| ORF | Nucleotide change | Amino acid change in Protein |
|---|---|---|
| 1a | 6172 C->T<br>10168 C->T<br>11775 A->G<br>12774 A->C | S1112F nsp3<br>S50F nsp5<br>I280V nsp6<br>M39L nsp9 |
| 1b | 19468 A->C | R489S nsp14 |
| Spike | 22119 A->G<br>23700 A->C | N222D<br>S749R |
| 4b | 26492 A->G | T134A |
| 5 | 26879-26896 ->G<br>27162 G->A | 15-224aa deletion<br>W108X |
| M | 27860 A->T | N3I |
| N | 28655 T->A | N30K |

**Figure S6. Mutations in mouse adapted MERS-CoV.** A) Mutations identified in 9 single plaque purified $MERS_{MA}$ viruses. For each coding region, the number of mutations observed is noted. *Missense or nonsense mutation, #Deletion. For additional details, see Table S1. B)

Schematic representation of the MERS-CoV genome and the location of mutations identified in $MERS_{MA}$ clone 6.1.2. Figure depicts sites in the genome where 12 non-synonymous mutations arose. Red symbols indicate sites of mutations. C) Description of the mutations present in $MERS_{MA}$ clone 6.1.2. An additional mutation was present in non-coding sequence (See Table S1).

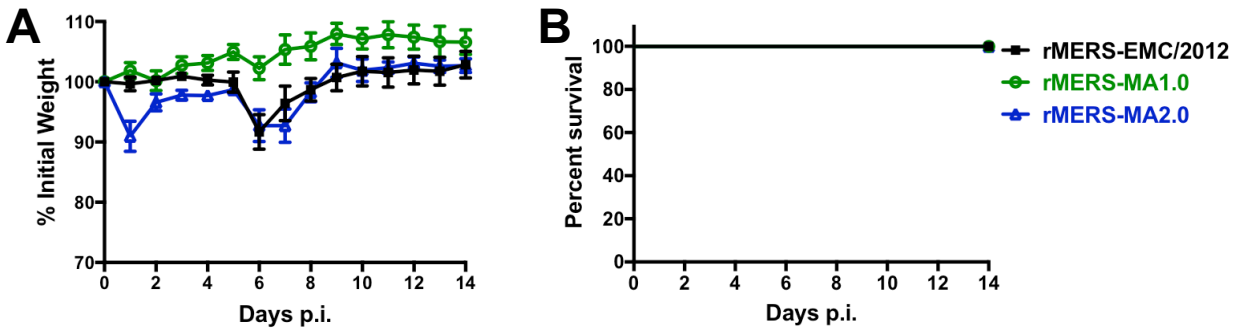


**Figure S7. Recombinant MERS-CoV with S protein mutations have reduced virulence in young mice.** Human DPP4 KI mice (age 6-8 weeks, male) received $10^5$ pfu of indicated recombinant MERS-CoV and were monitored daily for weight (A) and mortality (B) (n=5 per group). All 3 recombinant viruses caused minimal weight loss and no mortality in 6-8 week old hDPP4 KI mice.